# CORRELATION OF THEORY WITH EXPERIMENT FOR THE EFFECT OF FUEL ON PITCHING-TRANSLATION FLUTTER

A Thesis

Presented to

the Faculty of the Department of Engineering

University of Virginia

In Partial Fulfillment

of the Requirements for the Degree

Master of Applied Mechanics

by

John L. Sewall

April 1957

APPROVAL SHEET

This thesis is submitted in partial fulfillment of the requirements for the degree of Master of Applied Mechanics

Author

Approved:

Faculty Advisor

For Subcommittee

Chairman, Committee on Graduate Studies in Engineering

April 1957

ACKNOWLEDGMENT

The author feels highly indebted to Mr. Charles E. Watkins for his patient, helpful counsel as faculty advisor during the entire program of study and to Messrs. Harry L. Runyan, Donald S. Woolston, and Herbert J. Cunningham for their constructive suggestions in the writing of this thesis. In addition, the Langley Laboratory of the NACA is due a great deal of credit, not only for its permission to present this work, but also for the essential role it played in preparing the thesis in final form.

TABLE OF CONTENTS

CHAPTER

# LIST OF TABLES

## LIST OF FIGURES

## LIST OF SYMBOLS

| | |
|---|---|
| $a$ | dimensionless distance of elastic axis relative to midchord, positive aft |
| $A_o$, $A_n$ | initial and n-th amplitudes, respectively of a damped oscillation as given by equation (1) |
| $A_{ch}$, $A_{c\alpha}$, $A_{ah}$, $A_{a\alpha}$ | dimensionless aerodynamic coefficients used in flutter analysis (see appendix) |
| $A_{11}$, $B_{11}$, $D_{11}$, $E_{11}$ | elements of flutter determinant (see appendix) |
| $b$ | half-chord of wing, ft |
| $e_a$ | distance between wing quarter-chord and elastic axis, positive aft, ft |
| $e_T$ | distance between wing quarter-chord and volumetric centroid of external tank, positive aft, ft |
| $f$ | frequency, cycles per second |
| $f_h$ | uncoupled translation frequency, cycles per second |
| $f_\alpha$ | uncoupled pitching frequency, cycles per second |
| $g$ | value of damping coefficient which satisfies flutter determinant as a function of $1/k$ in flutter analysis (see Figure 9) |

| | |
|---|---|
| $g_h$, $g_\alpha$ | experimentally determined damping coefficients in translation and pitch, respectively |
| $h$ | vertical translation of elastic axis of wing section, or bending, positive down |
| $h(y,t)$ | translation (bending) component of flutter mode as defined by equation (5) |
| $i$ | $\sqrt{-1}$ |
| $\bar{I}_\alpha$ | mass moment of inertia of model in torsion about elastic axis, ft-lb sec$^2$ |
| $\bar{I}_{\alpha,Fluid}$ | effective mass moment of inertia of fluid about elastic axis, ft-lbs sec$^2$ |
| $\bar{I}_{\alpha,Solid}$ | mass moment of inertia of fluid considered as a solid about elastic axis, ft-lb sec$^2$ |
| $I_{T,\alpha}$ | volume moment of inertia of external tank about elastic axis, ft$^5$ |
| $I_z$ | linear momentum in vertical (or z-) direction (see appendix) |
| $k$ | reduced frequency, $b\omega/V$ |
| $k_h$ | bending stiffness of model, lb/ft |
| $k_\alpha$ | torsional stiffness of model, ft-lbs/radian |
| $L$ | Lagrangian (see appendix) |
| $\bar{m}$ | mass of model in torsion, lb-sec$^2$/ft |
| $\bar{m}'$ | mass of model per unit span in bending, lb-sec$^2$/ft |
| $\bar{m}_{Fluid}$ | effective mass of fluid, lbs-sec$^2$/ft |

| | |
|---|---|
| $\bar{m}_{Solid}$ | mass of fluid considered as a solid, lbs-sec$^2$/ft |
| $\bar{M}_a$ | aerodynamic moment acting on wing about elastic axis (see appendix) |
| $\bar{P}$ | aerodynamic force acting on wing (see appendix) |
| $q$ | generalized coordinate (see appendix) |
| $\delta_q$ | virtual displacement of generalized coordinate (see appendix) |
| $Q$ | generalized force (see appendix) |
| $r$ | outside radius of external tank, ft |
| $r_a$ | dimensionless radius of gyration of model about elastic axis, $\sqrt{\bar{I}_a/mb^2}$ |
| $R$ | ratio of dynamic response (amplitude) at resonance, $R_R$, to static response, $R_0$, at $\omega = 0$ (see equation (4)) |
| $s$ | wing span, ft |
| $T$ | kinetic energy (see appendix) |
| $U$ | potential energy (see appendix) |
| $V$ | airstream velocity, ft/sec |
| $V_{f,0}$ | experimental flutter speed of model in empty condition, used as a reference speed in Figures 6 and 8, ft/sec (see Table III) |
| $V_T$ | volume of external tank, ft$^3$ |

| | |
|---|---|
| $\delta W$ | virtual work (see appendix) |
| $x$ | chordwise coordinate of integration measured from wing quarter-chord, positive aft (see appendix) |
| $\bar{x}_{ea}$ | location of elastic axis of model from leading edge, per cent chord (see Table I) |
| $\bar{x}_{cg}$ | location of model center of gravity from leading edge, per cent chord (see Table I) |
| $x_a$ | location of model center of gravity relative to half-chord measured from elastic axis, positive aft |
| $\alpha$ | angle of pitch of wing section about elastic axis, positive leading edge up |
| $\alpha(y,t)$ | pitching (torsional) component of flutter mode as defined by equation (6) |
| $\gamma$ | $\frac{c}{c_{cr}}$ where $c$ is a viscous damping coefficient and $c_{cr}$ is the viscous damping coefficient for a critically damped oscillation, see equation (2) |
| $\kappa$ | ratio of mass of cylinder of air of radius $b$ to mass of model, $\pi\rho b^2 s$/total mass free to pitch (see also appendix) |

| | |
|---|---|
| $\omega$ | angular frequency, radians/sec |
| $\rho$ | air density, lb-sec$^2$/ft$^4$ |

Subscripts not otherwise identified:

| | |
|---|---|
| d | refers to torsional divergence (see appendix) |
| f | denotes flutter |
| h | refers to translational degree of freedom |
| j | denotes j-th degree of freedom |
| O | refers to tank-empty condition |
| o | refers to center of gravity (see appendix) |
| T | associated with external tank of model B |
| $\alpha$ | refers to pitching degree of freedom |

## SUMMARY

Analytical flutter studies were made for a two-dimensional fuel-loaded wing model, and the results are compared with experimental results for bending-to-torsion frequency ratios near 1. Water, simulating fuel, was carried externally in a geometrically scaled standard airplane fuel tank that was pylon-mounted a distance of about two and one-half times the tank radius beneath the wing. Some experimental results have been reported previously.

The calculated flutter speed results agreed well with experimental flutter speeds and flutter speed trends when the analysis employed effective values for the mass and mass moment of inertia together with slender-body air forces on the external tank, and when the combined structural and fluid damping was considered to be zero. However, use of even the smaller of the two damping coefficients in translation or pitch at zero airspeed resulted in poorer agreement between theory and experiment.

# CHAPTER I

## INTRODUCTION

General remarks. Problems of aircraft performance, stability, and control can be said to fall into one of two broad categories. One of these is the older study of the behavior of the aircraft and its various components in steady or quasi-steady motion, in which only the action of aerodynamic forces on rigid-body structures is considered. The other category, which has mushroomed in size and importance in recent years with the rapid developments in high-speed flight, is concerned with problems involving unsteady motion, wherein the time variable and the elasticity of structural elements must be taken into account.

Occupying a prominent position in the study of unsteady phenomena is an instability known as flutter. For the sake of enlightening the reader who may be unfamiliar with this instability, consider an elastic body in still air disturbed from equilibrium by a momentary external force. The resultant response is characterized by harmonic oscillations which progressively diminish in amplitude at a rate that is governed solely by the structural damping characteristics of the body. When the same body is similarly disturbed in a moving airstream, the oscillations may die out more quickly due to the retarding action caused by the

motion of the air across the body, or by what is known as aerodynamic damping. As the air velocity is increased, the rate of decay of these transient oscillations is also increased until, at a certain airspeed, it is possible for the rate of decay to reach a maximum. For a further increase in air velocity the damping rate may decrease and, at some critical velocity, become zero, at which time the oscillations are maintained at constant amplitude.

A situation of this kind characterizes a condition of flutter, in which the elastic and inertial forces, together with the structural friction forces, of the vibrating body interact with the oscillating forces of the air surrounding the body to produce the motion. It is possible to visualize such a condition by imagining the aerodynamic and mechanical forces to be arranged in the form of a triangle as shown in the following diagram[1] which also serves to locate flutter relative to certain other aircraft problems and fields of study:

[1] This concept was introduced by A. R. Collar in The Expanding Domain of Aeroelasticity, Journal of the Royal Aeronautical Society, Vol. L, pp. 613-636, August 1946.

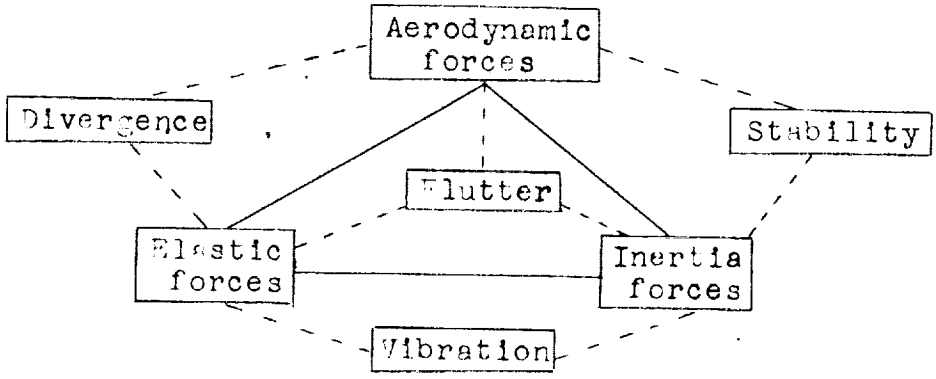


The dashed lines expanding and subdividing the triangle of forces into other triangles indicate what kind of forces are involved in these problems. Note that flutter lies in the center of the triangle, since all three types of forces[2] are involved, whereas the other problems, each dependent on just two types of forces, are located outside the triangle.

In the interaction of the aerodynamic, elastic, and inertial forces to produce flutter the energy required to maintain the borderline condition between damped and undamped oscillations is supplied entirely by the airstream rather than by any conventional system of externally applied forces. In this sense flutter is said to be self-excited. Due to the oscillations, the aerodynamic forces are not, as in the steady case, simple functions of circulation (which

---

[2] The structural damping or friction forces, previously mentioned, are here considered to be part of the elastic forces; for detailed consideration on this matter see chapter IV and the appendix.

determines the lift on the body) but are instead dependent on the instantaneous position of the body (i.e., angle of attack to the direction of the moving airstream). If the critical airspeed at which flutter occurs is exceeded, the aerodynamic forces are capable of overcoming the mechanical restoring forces (or elastic forces) stored in the structure to such an extent as to result in distortion or destruction of the body.

The role of flutter has become particularly conspicuous in the development of modern high-speed aircraft which are elastic bodies of considerable structural complexity, and in which many types of this instability can exist. Classical flutter theory for airplanes can treat the entire airplane as an elastic body whose motion is described by many degrees of freedom, or it can be confined to a portion of the airplane structure in which as few as two or three degrees of freedom may be sufficient to specify the motion adequately. Of the major aircraft components, those which still continue to receive the greatest attention form the lifting surfaces and control surfaces of the airplane. The flutter of these components involves the coupling of a large number of degrees of freedom including, principally, bending and torsional motions of a wing or tail surface together with the motions of their respective control surfaces.

Where bending and torsion are the only freedoms which interact to produce the motion of a wing (or stabilizer) at flutter, at any instant during the oscillation the torsional displacement from equilibrium lags the bending displacement. This lag in torsional displacement permits an additional lift force to be felt on every fore and aft strip of the wing, due to the torsional displacement, at any given bending displacement during the complete cycle of the coupled bending-torsion motion. In this manner the wing receives energy from the airstream.

As might be inferred from the foregoing remarks, the flutter characteristics of a wing depend largely on its mechanical properties. Of prime importance are not only the magnitudes but also the distributions of the elastic and inertial properties throughout the wing. With regard to the inertial properties, the effects of lumped or concentrated masses, representing such items as nacelles, external fuel tanks, and the like, have come to merit special study. This paper centers its attention on the effects an external wing fuel tank of varying mass and moment of inertia can have on classical flexure-torsion flutter.

Purpose of the investigation. It is the intent of this paper to compare theoretical results with experimental results obtained in the flutter of a simplified

two-dimensional model wing-tank configuration in which water, simulating fuel, was carried externally in a large streamlined tank mounted beneath the wing on a vertical strut, or pylon. The investigation is mainly concerned with how closely flutter speeds can be calculated for this configuration on the basis of effective or average values for the mass, mass moment of inertia, and fluid damping. In addition to those acting on the wing, the aerodynamic forces and moments acting on the tank are also included in the calculations, and the effect of these additional forces and moments on flutter is explored as a secondary objective of the project.

Importance of study. The occurrence of serious dynamic instabilities on a number of airplane carrying large quantities of fuel in the wings has stimulated investigations of the possible effects of the fuel motion on the aeroelastic behavior of the airplane. Of particular concern is the case of fuel carried externally in large streamlined tanks mounted either in the plane of the wing or on a vertical pylon so as to be offset from the wing. Investigations of the effect of fuel motion on aeroelastic instabilities have made use of both solid weights and fluid to simulate fuel. This dual representation is important because the inertial properties of the wing with fuel at rest (or imagined frozen) are known

to be different from the inertial properties of the wing with the fuel disturbed by an oscillatory motion such as flutter. It is further known that the amount of fluid effective as mass and mass moment of inertia in a tank undergoing translatory and pitching oscillations is generally less than the amount of fluid corresponding to the mass and moment of inertia of the same volume of fluid in the tank at rest. The validity of aeroelastic studies, such as flutter, therefore depends to a large extent on how well the dynamic behavior of the fuel is reproduced by means of effective values for the mass and mass moment of inertia.

Thesis organization. The next chapter reviews previous and related work, and succeeding chapters are devoted to the subject of the thesis itself. The experimental program is considered first in chapter III and the theoretical study in chapter IV. Results and correlation of theory with experiment are discussed in chapter V, and the entire investigation is summarized in chapter VI. Pertinent details relating both to theory and experiment are discussed in an appendix.

## CHAPTER II

## BACKGROUND

The exorbitant fuel requirements of current high-speed aircraft have forced designers not only to seek out every available space practicably suited to the location of fuel within the aircraft structure, but also to create additional fuel storage in large streamlined bodies mounted outside the airplane in such places as the wing tips or beneath the wings on vertical struts or pylons. While the shapes and sizes of these external stores have met aerodynamic and stability design requirements insofar as possible, the influence of fuel mobility on the airplane's dynamic behavior has not, in general, been adequately predictable for design purposes. Rather, instabilities due to fuel motion have been dealt with as they have arisen in completed configurations.[3] These difficulties have led to

[3] It is here noted that corrective measures for troubles traceable to flutter have been reported for a number of airplanes in investigations which have not only contributed knowledge toward a better understanding of the problem but have also been of such a character as to provoke further inquiry in areas where further work can still be profitably accomplished. The decision to omit specific reference to these cases in the present paper has therefore not been made with either the avowed or implied intention of minimizing their value. But in the interests of national security, investigations closely linked with most current military and naval airplanes are of necessity placed beyond the reach of the general reader. Formal citation of this work would, accordingly, impose a similar restriction on the availability of the present thesis which does not otherwise need to be so classified.

broader studies in which the dynamics of the fuel itself have been examined apart from the effects of fuel motion on the dynamic behavior of the airplane, or on one of its structural components.

A review of theoretical work on fluid dynamics reveals that the most significant contributions have appeared at widely separated intervals of time. Within the past seven or eight years a number of theoretical studies have been made of fluid motion in tanks of simple shapes. The favorite method of attack common to all of these studies has been the use of simple mechanical analogies to represent the complicated fuel motion. The essential elements of nearly all of these analogies rest on fundamental concepts of potential flow theory as given by Sir Horace Lamb.[4] On the basis of the classic mathematical derivations of this eminent writer, Graham[5] in 1951 presented expressions for the forces produced by fluid oscillations in a stationary rectangular tank, in which the fluid is replaced by a fixed mass together with an equivalent pendulum to represent small oscillations of the

---

[4] Sir Horace Lamb, Hydrodynamics, 6th ed., Dover Publications (New York), 1945.

[5] E. W. Graham, The Forces Produced in a Rectangular Tank, Douglas Aircraft Co., Inc., Report SM-13748, April 1951.

free fluid surface. This work has been extended in a subsequent paper[6] in which mathematical expressions are developed for the response of fluid in a rectangular tank to simple harmonic motions in translation, pitch, and yaw. In this case the equivalent mechanical system consisted of a fixed mass, and the free surface disturbances were represented by a combination of linear spring-mass oscillators. Further study of the use of the equivalent pendulum to represent the fluid's dynamic behavior has been made by Lorell,[7] who has shown this analogy to be a good approximation when the fluid is forced at frequencies close to its natural fundamental frequency.

Whereas feasible theoretical solutions for the problem of fluid mobility fall within the domain of small oscillations, experimental inquiries have dealt with turbulence and splashing in the search for quantitative information on the mechanical properties of the fluid. Until recently, general information of this kind had been conspicuously lacking. Within the past few years this void has been partially,

---

[6] E. W. Graham and A. M. Rodriguez, The Characteristics of Fuel Motion Which Affect Airplane Dynamics, Douglas Aircraft Co., Inc., Santa Monica, Calif., Report SM-14212, November 27, 1951.

[7] Jack Lorell, Forces Produced by Fuel Oscillations, Jet Propulsion Laboratory, California Institute of Technology, Progress Report No. 20-149, October 16, 1951.

though substantially, filled in three studies involving the use of single-degree-of-freedom systems. Using two simplified model beam-tip tank systems, Merten and Stephenson[8] have obtained data on the effective weight and damping of sloshing fluid in cylindrical and rectangular tanks at the free ends of cantilever beams subjected to bending motion. For a number of different fluids tested, the effects of fluid density and tank fullness were found to be significant, whereas no appreciable effects of fluid viscosity or tank shape were discernible. Subsequently, Widmayer and Reese[9] in a similar investigation have measured effective moments of inertia and have demonstrated nonlinear damping characteristics in tip tanks subjected to pitching oscillations. These experiments showed the effective fluid moments of inertia to be essentially independent of tank fullness and tank size for centrally mounted tanks. In addition, the ratio of fluid to solid moment of inertia increased with increasing fineness ratio, closely following trends predicted

---

[8] Kenneth F. Merten and Bertrand H. Stephenson, Some Dynamic Effects of Fuel Motion in Simplified Model Tip Tanks on Suddenly Excited Bending Oscillations, Langley Aeronautical Laboratory, NACA TN 2789, September 1952.

[9] Edward Widmayer, Jr., and James R. Reese, Moment of Inertia and Damping of Fluid in Tanks Undergoing Pitching Oscillations, Langley Aeronautical Laboratory, NACA RM L53E01a, June 11, 1953.

by theoretical solutions for full rectangular and ellipsoidal tanks.[10] Further experiments[11] have shown, among other things, a pronounced effect of tank fullness on the effective moment of inertia of fluid in pylon-mounted tanks.

The influence of fuel mobility on the dynamics of the entire airplane has been considered particularly important in both stability and flutter. In an extensive theoretical stability study, Schy[12] has derived the general equations of motion of an airplane carrying fuel in a number of tanks. The fuel motion is approximated by the motion of simple pendulums, and the analysis was applied both to a current high-speed airplane and to a simplified free-flying model carrying two large spherical tanks in the fuselage. It was shown from these calculations that airplane motion can be greatly affected by the ratio of natural fuel frequency to

---

[10] John W. Miles, An Analogy Among Torsional Rigidity, Rotating Fluid Inertia, and Self-Inductance for an Infinite Cylinder, Journal of Aeronautical Sciences, Vol. 13, No. 7, July 1946, pp. 377-380.

[11] James R. Reese and John L. Sewall, Effective Moment of Inertia of Fluid in Offset, Inclined, and Swept-Wing Tanks Undergoing Pitching Oscillations, Langley Aeronautical Laboratory, NACA TN 3353, January 1955.

[12] Albert A. Schy, A Theoretical Analysis of the Effects of Fuel Motion on Airplane Dynamics, NACA TN 2280, January 1951. (Superseded by NACA Report 1080, 1952.)

natural airplane frequency particularly when this frequency ratio is unity. The possibility that fuel turbulence might have a stabilizing influence on the airplane motion is also discussed. Luskin and Lapin[13] have also studied the effects of fuel on rigid airplane stability by means of the pendulum analogy and have been specifically concerned with the effects of fuel on longitudinal motion of the airplane.

The effect of fluid oscillation and splashing on flutter has been the object of investigations similar to those devoted to trouble-shooting but generally of somewhat broader scope, in the sense that they deal more with the symptoms of flutter troubles and less with the urgent search for cures of these troubles. These investigations have in common the use of models in which provision has been made for the variation of significant parameters. One such study is an experimental investigation of flexure-aileron flutter on a simplified model wing equipped with an integral tank in which water was used to simulate fuel.[14] The tank was not equipped with baffles, but the effect of baffles was

---

[13] Harold Luskin and Ellis Lapin, An Analytical Approach to the Fuel Sloshing and Buffeting Problems of Aircraft, Douglas Aircraft Co., Inc., Report SM-14068, June 1951.

[14] G. Scruton, Wing Flexure-Aileron Flutter Tests on a Model R.A.C. Wing Type 167, Aeronautical Research Council, R. and M. No. 2480, October 16, 1944.

achieved through the use of solid weights whose inertial properties approximated those of the water. Comparison of flutter speeds obtained using fluid with those found using equivalent solid weights indicated that the fluid loading condition improved the flutter characteristics, that is, somewhat higher flutter speeds were obtained. The approach of the inertial properties of fuel in a highly baffled tank to the inertial properties of equivalent solid weights has been demonstrated by Beckley and Johnson[15] in flexure-torsion flutter tests on a model wing equipped with a vertically offset (or underslung) tip tank, in which the fuel cavity was divided into a number of sealed compartments. These experiments, which also included tests with weights simulating the fuel as a solid, revealed gradual changes in flutter speed with variations in the chordwise location of the tank and in the amount of fluid, but no appreciable effect attributable to fuel motion was found. More recent studies by Gayman[16] have embraced a somewhat similar test program on a semiwing flutter model with various centrally

---

[15] Lawrence E. Beckley and H. Clay Johnson, Jr., An Experimental Investigation of the Flutter of a Tapered Wing With Simulated Engines, Tip Float and Tip Tank. (For the Bureau of Aeronautics, U. S. Navy), Massachusetts Institute of Technology, Contract No. NOa(s)7493, November 15, 1947.

[16] William H. Gayman, An Investigation of the Effect of a Varying Tip-Weight Distribution on the Flutter Characteristics of a Straight Wing, Journal of the Aeronautical Sciences, Vol. 19, No. 5, May 1952.

mounted tip tanks having single-compartment cylindrical fuel cells. Here, although practical limitations inherent in the test apparatus precluded flutter experiments with fluid in the tanks, the simulation of fluid inertial properties by means of lead weights was determined on a rational basis which was supported by measurements of the pitching moments of inertia of water in a model fuel cell. The wing was dynamically scaled from the wing of a current fighter airplane so as to flutter within the speed range of the test facility used, and the investigation was mainly concerned with the antisymmetric flutter mode. Results of these flutter tests with fuel simulated in the manner described above revealed a pronounced effect on flutter speed over a limited range of fuel loading for which the ratio of bending-to-torsion frequency ratio was very nearly one. In one series of tests, for example, the flutter speed was abruptly reduced by as much as 50 per cent for a decrease in fuel loading from 67 per cent to 56 per cent full.

A similar frequency ratio effect has also been found in a recent experimental investigation[17] for a two-dimensional wing configuration equipped with a vertical strut or pylon to which was mounted, beneath the wing, a

---

[17] James R. Reese, Some Effects of Fluid in Pylon-Mounted Tanks on Flutter, Langley Aeronautical Laboratory, NACA RM L55F10, July 19, 1955.

large streamlined tank that could be filled with fluid or fitted with solid weights and baffles. The results of these tests demonstrated the usefulness of certain previous fuel dynamics studies[18] by showing that when a given volume of fluid in the tank was replaced by solid bodies whose inertial properties were equal to effective values of these properties for the same volume of oscillating fluid, the model fluttered at the same speeds as it did with the fluid. The present investigation goes one step further by correlating these experimental flutter results with the results of flutter calculations for all fluid loading conditions from 0 to 100 per cent full. The simplicity of the model and apparatus tends to isolate the effects of fuel motion on flutter by minimizing or ruling out altogether certain complicating aerodynamic and structural effects inherently involved in more realistic wing structures. Specifically, the configuration is particularly well-suited to the simplest application of flexure-torsion flutter theory because the assumption of two-dimensional air flow over the wing is more fully satisfied and because the structural behavior of the wing is simple enough to be adequately represented by just two degrees of freedom, namely, vertical translation (simulating bending) and pitch (simulating torsion).

---

[18] Merten and Stephenson, Widmayer and Reese, and Reese and Sewall, op. cit.

# CHAPTER III

## EXPERIMENTAL PROGRAM

This investigation was initiated by a series of experiments designed to find out how certain properties important in aircraft vibration and flutter were affected by the erratic, sloshing motion of fuel located in a major aircraft structural component, such as the wing. These experiments were implemented by the use of a simplified two-dimensional wing apparatus in which a large streamlined tank capable of holding fluid was pylon-mounted beneath a semi-rigid, untapered wing mounted on bending and torsional springs located outside an airstream. The vibratory characteristics of the model were measured both in still air and at airspeed, during flutter, for a complete range of fluid loadings from empty to full. Most of the results of the experimental program have been previously reported,[19] and some of the results needed for correlation with theoretical results are reported again in this chapter and supported by a detailed description of pertinent features and details of the experiments. In addition, some previously unpublished experimental results of secondary importance are included.

---

[19] Reese, op. cit., see chapter II.

## MODEL AND APPARATUS

The wing-tank configuration used in this investigation is shown in Figure 1. Fluid was carried externally in a geometrically scaled standard airplane fuel tank that was pylon mounted a distance of about two and one-half times the tank radius beneath the wing. The wing was of aluminum alloy construction, including a 0.032-inch skin, except for an internal hardwood core formed to the airfoil contour. The center of the tank pylon was located above the center of the tank midsection and was fastened to the wing through a bracket which permitted chordwise variation of the fore and aft center-of-gravity position of the pylon-tank assembly. Tables I and II list some additional data for the model.

A schematic view of the apparatus is shown in Figure 2. Arrows indicate the directions of translational and pitching degrees of freedom restrained by bending (translational) and torsional (pitching) springs which were mounted outside the test section of the Langley 2- by 4-foot flutter research tunnel. The stiffnesses of one set of bending and torsional springs were selected so that the uncoupled wing bending-to-torsion frequency ratios for the model containing fuel passed through unity with increasing tank fullness. Values for these spring stiffnesses are given in Table I. A second set of spring stiffnesses listed

TABLE I.- CERTAIN MODEL PARAMETERS

| | |
|---|---|
| b, ft | 0.5 |
| s, ft | 2.0 |
| Airfoil section | NACA 65-010 |
| Maximum fuel depth, in. | 4.19 |
| Maximum external diameter of tank, in. | 4.25 |
| $\bar{x}_{ea}$, per cent chord | 40 |
| $\bar{x}_{cg}$, per cent chord | |
| Tank empty | 43.9 |
| Tank full | 39.5 |
| $k_h$, lb/ft | 2015 |
| | 3340 |
| $k_\alpha$, ft-lb/radian | 343.5 |
| | 204.1 |
| $\bar{m}'$, lb-sec$^2$/ft | |
| Tank empty | 0.404 |
| Tank full | 0.712 |
| $\bar{m}$, lb-sec$^2$/ft | |
| Tank empty | 0.2285 |
| Tank full | 0.536 |
| $\bar{I}_\alpha$, ft-lb sec$^2$ | |
| Tank empty $\left(\bar{I}_{\alpha,0}\right)$ | 0.0309 |
| Tank full | 0.1805 |
| $f_h$, cycles per second | |
| Tank empty | 11.2 |
| Tank full | 8.36 |
| $f_\alpha$, cycles per second | |
| Tank empty | 16.7 |
| Tank full | 7.22 |
| $g_h$, empty | 0.009 |
| $g_\alpha$, empty | 0.018 |

TABLE II.- CERTAIN GEOMETRIC PROPERTIES OF EXTERNAL TANK

(a) Tank ordinates.

| Distance from nose of tank (in.) | r (ft) |
|---|---|
| 0 | 0 |
| 1.09 | .0658 |
| 2.03 | .1016 |
| 3.41 | .1358 |
| 4.54 | .1542 |
| 5.88 | .1684 |
| 8.58 | .1750 |
| 9.875 | .1770 |
| 18.33 | .1770 |
| 20.47 | .1716 |
| 23.77 | .1275 |
| 27.18 | .0642 |
| 30.3 | 0 |

(b) Volumetric properties.

| Tank center of gravity (per cent chord) | $e_T$ (ft) | $V_T$ $(ft)^3$ | $I_{T,a}$ $(ft)^5$ |
|---|---|---|---|
| 30 | 0.01584 | 0.05415 × π | 0.01662 × π |
| 40 | .1158 | ↓ | .01570 |
| 50 | .2160 | | .01586 |
| 60 | .3160 | | .01714 |

in the table yielded frequency ratios greater than one for the model fluttered without fuel over a range of fore and aft center-of-gravity positions of the pylon-tank assembly from 30 to 60 per cent of the wing chord aft of the wing leading edge.

The model was fluttered in air at atmospheric pressure with fuel loads simulated by water and by solid weights. The solid weights were mounted inside the tank.

## EFFECTIVE INERTIAL PROPERTIES OF THE FUEL-LOADED MODEL

The apparatus was equipped with restraints so that the model could be excited, or vibrated, in one degree of freedom independent of the other. This was an important feature because it permitted the measurement of uncoupled frequencies in either pure translation or pure pitch.

These frequencies were obtained by instantaneously releasing the model from initial amplitudes. The resulting responses were picked up by resistance wire strain gages mounted on the bending and torsional springs as indicated in Figure 2. The strain-gage signals felt by these responses were fed through a system of electrical bridges and amplifiers into a recording oscillograph in which the signals were traced on photographic paper. The paths of the strain-gage signals varied sinusoidally with the length of paper

(corresponding to increasing time), and the frequencies were determined by counting the number of sinusoidal cycles for a particular time interval.

The frequencies measured in this manner were used to determine the amount of fluid effective as mass and mass moment of inertia during flutter by application of essentially the same technique as that used in previous experimental investigations of these properties.[20] In order to determine the best approximations to effective values of mass and moment of inertia at flutter for the model containing fluid, the frequencies read on the zero-airspeed vibration records covered the same range of amplitudes encountered during flutter.

Within reading accuracy these frequencies remained very nearly constant over the time interval and corresponding amplitude range chosen in each case. This frequency invariance should not, however, be regarded as being generally characteristic of vibrating configurations containing fluid free to slosh or splash. Indeed, for one of the models used in the experiments of Merten and Stephanson,[21] there

---

[20] Merten and Stephanson, Widmayer and Reese, and Reese and Sewall, op. cit., chapter II.

[21] Ibid.

existed an appreciable cycle-by-cycle frequency variation throughout the time history of oscillations in bending (equivalent to vertical translation) for each test with a simple cylindrically shaped tank partly full. Although it is not readily apparent why this behavior was not encountered in the experiments reported in this thesis, a possible explanation is that due to the cone-shaped ends of the external tank, the fluid may tend to follow the vertical motion of the tank, whereas in the cylindrically shaped tank the fluid is free to move along the straight vertical end boundaries independently of the motion of the tank. Further studies would, of course, be required to determine whether or not this reasoning is valid.

It is intended by repeated reference to effective values to emphasize the fact that the mass and moment of inertia of an oscillating tank containing fluid are different from the mass and moment of inertia of the tank containing the same volume of fluid at rest, or in a solid condition. Indeed it has been shown[22] that effective values of these properties are generally less than the corresponding "solid values," as one might intuitively expect them to be.

---

[22] Ibid.

The center-of-gravity variation with tank fullness is shown in Figure 3. This variation is based on experimental values obtained for the extremes of tank fullness represented by the symbols, and the straight line connecting the symbols indicates that linear interpolation was employed to obtain centers of gravity for intermediate fullnesses.

Figure 4 shows the variation of effective mass and Figure 5 the variation of effective mass moment of inertia with tank fullness. The data in both Figures have been referred to the mass and moment of inertia of the tank-empty condition for the model. Numerical values beside the points on the dotted curves and lines give the amount of fluid effective as mass and moment of inertia during translatory and pitching oscillations, respectively. In obtaining the data in Figure 4 the variation of the measured translational frequency with mass was first established for several different solid weights mounted inside the empty tank. The effective mass of the model containing a given amount of fluid is then the empty mass plus the equivalent solid mass corresponding to the translational frequency measured for that fluid load.

The method of determining the effective moments of inertia presented in Figure 5 is similar to that used for determining the effective masses presented in Figure 4.

The solid weights mounted inside the empty tank were designed to the solid moments of inertia of the fuel for tank fullnesses up to 100 per cent, and the variation of measured pitching frequency with these solid inertias was established. The effective moment of inertia of the model containing a given amount of fluid was then found by adding the model-empty moment of inertia to the equivalent solid moment of inertia corresponding to the measured pitching frequency for that fluid load. Values on the solid curve in Figure 5 were calculated by numerically integrating the moment of inertia of the fluid over the space bounded by the internal tank length, the free surface, and the internal tank contours for all fullnesses.

## METHODS OF MEASURING DAMPING OF MODEL

The damping of the model with and without fluid in the tank was measured by two different methods. One of these was the so-called "decrement" method which was used to measure the damping of the model-empty and model-full conditions, and the other was the frequency-response method which was used to measure the damping for all partially full conditions.

Progressively diminishing amplitudes of successive cycles of oscillation characterize vibrations produced by the instantaneous release of an elastic body from an initial amplitude and permit an evaluation of damping of that body by means of the decrement method. In this investigation the evaluation was based on the commonly used viscous damping concept (i.e., damping force proportional to velocity) in which the envelope of the decaying amplitudes in a given oscillation leads to the simple expression

$$g_j = \frac{1}{n\pi} \log \frac{A_o}{A_n} \qquad (1)$$

where $g_j$ is the structural damping coefficient in the j-th mode or degree of freedom and $\log \frac{A_o}{A_n}$ is the natural logarithm of the ratio of the initial amplitude $A_o$ to the final amplitude $A_n$ after $n$ cycles of oscillation. This expression usually known as the logarithmic decrement, should be applied to portions of the recorded response for which the values of $A_o$ to $A_n$ fall in a straight line when plotted to a logarithmic scale against cycle number.

Damping based on the frequency-response method is determined by forcing an elastic body at a frequency equal to its natural frequency. Using the equation of a single-

degree-of-freedom system subjected to a forced vibration, Scanlan and Rosenbaum[23] have shown that

$$\gamma = \frac{c}{c_{cr}} = \frac{1}{2} \frac{\frac{\Delta\omega}{\omega_R}}{\sqrt{R^2 - 1}} \qquad (2)$$

where $\gamma$ is the ratio of the viscous damping coefficient for the oscillatory case to the critical viscous damping coefficient, or the coefficient corresponding to the condition which separates oscillatory motion from nonoscillatory motion. The quantity $R$ is the ratio of the peak response (or amplitude) of the system at resonance (i.e., when the forcing frequency equals the natural frequency) to the response for a forcing frequency less than the resonant frequency. The term $\Delta\omega$ is the frequency difference which, on a plot of response against frequency, gives the approximate width of the response peak in the vicinity of resonant frequency $\omega_R$. Making use of the relations $\omega_R - \omega_1 = \frac{\Delta\omega}{2}$ and $\gamma = 2g_j$, also derived by these writers,[24] equation (2) may be written as follows:

---

[23] Robert H. Scanlan and Robert Rosenbaum, Introduction to the Study of Aircraft Vibration and Flutter, MacMillan Co., 1951, chapter III.

[24] Loc. cit.

$$g_j = \frac{1}{4} \frac{\frac{\Delta\omega}{\omega_R}}{\sqrt{R^2 - 1}} = \frac{1}{\sqrt{R^2 - 1}} \qquad (3)$$

where $R = \frac{R_R}{R_o}$, or the ratio of the dynamic response at resonance to the static response for $\omega_1 = 0$. For large values of $R$ this expression reduces to

$$g_j \cong \frac{1}{R} \qquad (4)$$

The damping coefficients for intermediate tank fullnesses were determined from this relation.

## FLUTTER TESTING TECHNIQUE

The vibratory characteristics of the wing-tank system in a moving airstream were studied in the Langley 2- by 4-foot flutter research tunnel at atmospheric pressure. The model was mounted horizontally in the test section as shown in Figure 2. The prime object of these tests was to find the flutter speed, as defined in the first chapter, for several tank fuel loads ranging from empty to full.

The flutter speed for each fuel load was determined from the aerodynamic conditions in the tunnel. The frequency at flutter is the same for both translation (bending) and pitching (torsion) components of the oscillation and was measured from the strain-gage traces on the oscillograph records. Because of the suddenness and violence with which flutter is expected to occur, the critical flutter speed must be established and all the necessary information recorded as instantly as possible. The airspeed is then quickly reduced in an effort to save the model from destruction and avert damage to the wind tunnel. This quick action was imperative in the present investigation whenever the model was fluttered without fluid but was unnecessary in the tests with fluid in the tank due to the unusual nature of the flutter response during these tests.

Flutter data were obtained with the center of gravity of the pylon-tank assembly located in four different positions ranging from 30 to 60 per cent of the wing chord aft of the wing leading edge. For all flutter tests with fluid in the tank, this position was fixed at 40 per cent of the wing chord aft of the wing leading edge.

The flutter test procedure for each fuel loading condition may be summarized as follows:

1. At zero airspeed the translation and pitching natural frequencies of the model were obtained by instantaneously releasing it from initial amplitudes as described in a previous section.

2. Next the tunnel airspeed was increased steadily until a flutter condition was attained. For this model it was necessary to disturb the model during this speed increase by frequently tapping or striking part of the apparatus outside the airstream in order to eliminate the influence of friction in the bearing (see Figure 2) on flutter. This part of the procedure was necessary in order to obtain repeatable flutter speeds.

3. As soon as flutter was recognized, the tunnel aerodynamic conditions needed to determine flutter speed and air density were recorded and the bending and torsional oscillations reproduced on the recording oscillograph.

4. With the desired information obtained the tunnel airspeed was quickly reduced in cases of violent flutter. For cases of mild flutter, in which the flutter amplitudes were limited by fluid sloshing, it was possible to increase the airspeed into the unstable region and repeat the previous step.

## EXPERIMENTAL RESULTS

The experimental results reported herein supplement those reported by Reese[25] for the tank without baffles. These results are listed in Table III. As previously noted, the damping coefficients for all partially full conditions were determined from frequency-response curves obtained at zero airspeed. The corresponding translational and pitching flutter amplitudes are also listed in the Table.

The flutter speeds given in the Table are shown, referred to the tank-empty flutter speed, in Figure 6 as functions of the tank fullness. Values of the frequency ratio $\frac{\omega_h}{\omega_\alpha}$ are shown alongside the data points. The significance of these values with regard to fluid damping has been discussed previously[26] and is mentioned again in a subsequent section of the present paper. This strong frequency-ratio effect on flutter speed is not only of practical importance in realistic configurations but has also been encountered in such configurations, as, for example, in the case of the dynamically scaled wing-tip tank model of Gayman's[27] investigation.

---

[25] Reese, op. cit.

[26] Ibid.

[27] William H. Gayman, op. cit., chapter II.

The limiting effect of fluid turbulence on flutter amplitudes has also been discussed previously[28] and is examined further in the present paper. As Table III(a) shows, the model fluttered over a wide speed range and a correspondingly limited amplitude range for all partially full conditions. Notice, however, that the flutter amplitudes consistently increased with further increase of airspeed for tank fullnesses ranging from 25 to 75 per cent full, whereas, for greater fullnesses the amplitudes tended to reach a peak and thereafter consistently decreased with increasing speed. This behavior may be seen more clearly in Figure 7 in which the translational and pitching components of the flutter amplitudes are shown as functions of airspeed for the 85, 90, and 95 per cent full conditions. Values of the damping coefficients $g_h$ and $g_\alpha$ corresponding to the flutter amplitudes are shown beside the data points. As noted in Table III(a) (footnote b) with the tank 95 per cent full, the model essentially stopped fluttering when the pitching amplitude became 0° and the translational amplitude was barely visible. Thus, there appears to be a closed or bounded flutter region for this case. On the basis of this experience and of the pitching amplitude trends for the other two fuel loads, it was possible by extrapolation

---

[28] Reese, op. cit.

(indicated by the broken curve) to establish closed flutter regions for these cases also. The upper flutter speed boundary determined in this manner is shown in Figure 6 in terms of the tank-empty flutter speed and can be seen to be anywhere from 62 to 97 per cent higher than the lower flutter speed boundary.

In addition to the fuel load studies, flutter tests were also conducted for the empty external tank located at a few other chordwise center-of-gravity positions. A different set of bending and torsional springs was used, and the frequency ratios obtained were greater than one. The results of these tests are given in Table III(b) and shown as a function of $x_a$ in Figure 8. The range of $x_a$ values corresponds to a range of tank c.g. positions from 30 to 60 per cent of the wing chord aft of the wing leading edge. The damping coefficients are based on logarithmic decrements of the amplitude decays corresponding to the natural frequencies listed in the table. As was to be expected, the range of forward center-of-gravity positions at which flutter could be obtained was limited by the divergence speed boundary.

# CHAPTER IV

## ANALYTICAL STUDY

The experimental work reported in the preceding chapter was followed by an analytical study which was undertaken for the purpose of determining how closely the experimental flutter speeds and flutter frequencies of the simplified wing-tank configuration could be reproduced by application of classical bending-torsion flutter theory. The chief feature of this application was the manner in which the dynamic behavior of the fuel was accounted for. This was done by using effective values to approximate the inertial properties of the fuel (in a fluid condition) and by introducing combined structural and fluid damping according to a commonly used assumption. The method of flutter analysis used was the so-called Rayleigh-Ritz method in which the highly coupled flutter motion is represented by a combination of series expansions involving degrees of freedom given by the natural modes of vibration in bending and torsion. The aerodynamic forces and moments assumed to be acting on the model at flutter were obtained by simply adding the forces and moments derived for the wing on the basis of two-dimensional incompressible flow theory to those derived for the external tank by application of slender-body theory. The method and application of the flutter analysis together with the results of flutter

calculations are presented and discussed in this chapter. Important details of the analysis are given in an appendix.

## METHOD AND APPLICATION OF THE ANALYSIS

As previously noted, the flutter motion (or flutter mode as it will be termed hereafter) is approximated by a combination of the natural modes of vibration in bending and torsion. With the use of generalized coordinates this combination may be written as follows for the bending and torsional components of the flutter mode at a particular spanwise position y:

$$h(y,t) = \sum_{j=1}^{\infty} h_j(t)\bar{h}_j(y) \qquad (5)$$

and

$$\alpha(y,t) = \sum_{j=1}^{\infty} \alpha_j(t)\bar{\alpha}_j(y) \qquad (6)$$

where $h_j(t)$ and $\alpha_j(t)$ are generalized coordinates of the j-th mode and express, respectively, the vertical displacement of a point on the torsional or rotation axis[29] and the angular displacement or rotation about that axis. The functions $\bar{h}_j(y)$ and $\bar{\alpha}_j(y)$ are modal functions which must be multiplied by the corresponding generalized coordinates

[29] This is more often referred to as the elastic axis.

in order to locate the instantaneous position of $y$ in space. For a given elastic structure the distributions of these functions along the span give the distortion or shape of the structure in the j-th mode.

As is indicated in Figure 2 for the model used in this investigation, the wing was stiff enough in the spanwise[30] direction to be considered rigid or undeformable in that direction. Hence, $\bar{h}_j(y)$ and $\bar{\alpha}_j(y)$ could be each taken equal to unity. Moreover, for all practical purposes the bending and torsional springs each behaved as single-degree-of-freedom systems so that $j$ in the foregoing equation could also be taken as one.[31] With these simplifications the flutter mode was represented by

$$h(y,t) = h_1(t) \equiv h_1 \tag{5a}$$

$$\alpha(y,t) = \alpha_1(t) \equiv \alpha_1 \tag{6a}$$

---

[30] The approach to chordwise rigidity is more or less implied in the designation of $\bar{\alpha}_j$ as a function only of the spanwise direction.

[31] With respect to the bending straps shown in Figure 2, this statement may not be strictly correct since these straps are cantilever beams for which an infinite number of vibration modes exist. However, it was felt that the frequencies of modes higher than the first were so far beyond the range of experimental flutter frequencies as to have a negligible effect if included in the flutter calculations.

The equations of motion of the model at flutter were obtained for these two coordinates from Lagrange's equations as is shown in the appendix.

The generalized forces and moments are given by the oscillatory aerodynamic forces and moments assumed to be acting on the system at flutter. Because the wing was untapered in the spanwise direction, the aerodynamic forces and moments acting on the wing could be more truly reproduced by use of the two-dimensional incompressible flow coefficients derived in terms of Bessel functions by Theodorsen.[32] Oscillating aerodynamic forces and moments acting on the external tank were taken into account by application of slender-body theory to obtain expressions from which aerodynamic coefficients for the tank were derived as shown in the appendix. The term "slender-body" identifies a basic assumption used in the derivation of these tank forces and moments, namely, that the cross flow, or flow between and parallel to

---

[32] See Theodore Theodorsen, General Theory of Aerodynamic Instability and Mechanism of Flutter, NACA Rep. 496, 1935.

planes normal to the airstream, is considered two dimensional.[33] The aerodynamic coefficients for the wing were simply added to the aerodynamic coefficients for the external tank to obtain the aerodynamic coefficients for the complete configuration.

From solutions of the equations of motion for the condition of simple harmonic motion is obtained the determinantal stability equation which leads to the analytical flutter speed and flutter frequency, as is also shown in the appendix. This stability equation yields a polynomial in $\frac{1}{\omega^2}$ with complex coefficients, $\omega$ being the frequency. The aerodynamic terms included in these coefficients are computed for a particular value of the reduced wave length $\frac{1}{k} = \frac{V}{b\omega}$. Accordingly, the roots $\frac{1}{\omega^2}$, which are in general complex, correspond to a particular value of $\frac{1}{k}$. If the flutter frequency is required to be a real and positive quantity, then the stability equation may be separated into two

---

[33] This assumption is basic to the impulse-momentum method, due to Munk, for determining aerodynamic forces and moments acting on a slender body (that is, a body having a high fineness ratio). This method is dependent on the concept of impulsive pressure for determining the force imparted to fluid surrounding a body due to a momentary acceleration of the body in the direction of the force. These matters are reviewed at length by Bisplinghoff, Ashley, and Halfman in chapters 5(pp. 200-204) and 7(pp. 418-420) of Aeroelasticity, Addison-Wesley Publishing Company, Inc., 1955.

distinct equations, one real and one imaginary. The value of $\frac{1}{k}$ which results in a real and positive value of $\frac{1}{\omega^2}$ that satisfies both real and imaginary equations determines the flutter speed and flutter frequency. As may be evident, this is inherently a trial-and-error procedure, usually requiring several choices of $\frac{1}{k}$, for each of which the aerodynamic terms are computed and the corresponding stability equation obtained.[34] Since the roots of the stability equation are complex, an alternative and widely used approach to the solution involves the introduction of an additional unknown which may be chosen from among the various parameters appearing in the equilibrium equations of motion.

In the present application of flutter theory the flutter frequency parameter $\frac{1}{\omega^2}$ was combined with a theoretical damping coefficient $g$ to form the complex quantity $\Omega = \frac{1}{\omega^2}(1 + ig)$. Solutions for $\Omega$ were thus formed for each $\frac{1}{k}$ and values of $\omega$ and $g$ were determined. In this

---

[34] Details of this method of solution for flutter are given by Theodore Theodorsen and I. E. Garrick in Mechanism of Flutter, A Theoretical and Experimental Investigation of the Flutter Problem, NACA Rept. No. 685, 1940.

procedure, advanced by Smilg and Wasserman,[35] the assumption is made in determinant elements along the principal diagonal that $g_h = g_\alpha = g$, where for speeds below flutter $g$ is negative and may be interpreted as indicative of the amount of negative damping energy required to cause flutter at a particular speed (or at a particular $\frac{1}{k}$). Consistent with this viewpoint, a flutter condition is obtained when $g = 0$, and the oscillations are self-maintained at constant amplitude, corresponding to a borderline condition of neutral stability. For values of $\frac{1}{k}$ greater than this critical point, the sign of $g$ changes from negative to positive, proceeding into a region of divergent or undamped oscillations for a condition wherein the energy of such oscillations is capable of causing structural distortion or failure. The manner in which $g$ changes with airspeed, or an airspeed parameter such as $\frac{V}{b\omega_\alpha}$, may be seen more clearly in Figure 9 for some of the flutter calculations performed in this study. Attention is directed to the solid curves, and, with the exception of Figure 9(g), only the portions of the curves in the vicinity of a flutter solution (i.e., at intersections with $g = 0$) are shown.

---

[35] Benjamin Smilg and Lee S. Wasserman, Application of Three-Dimensional Flutter Theory to Aircraft Structures, AFTR 4798, Materiel Div., Army Air Corps., July 9, 1942.

The dynamic behavior of the fuel was represented in the flutter calculations by means of effective values of mass and mass moment of inertia given in Figures 4 and 5 and the measured damping coefficients given in Table III. The validity of using effective values for the inertial properties has been established experimentally in previously referenced work[36] in which flutter speeds of the model containing fluid were generally duplicated when the fluid was replaced by solid weights equivalent to the fluid in effective mass and mass moment of inertia.

Solution of the stability equation by means of the dual unknown approach including damping involves one more concept that is also widely used. This concept regards the measured structural damping coefficients as zero airspeed as indicative of the ability of a given configuration, through its inherent damping energy, to change the flutter speed from that corresponding to $g = 0$. In this sense the measured $g_h$ or $g_a$ is considered as positive and as providing a flutter speed margin whose breadth depends both on the trend of the theoretical $g$ value with flutter speed and also on the magnitude of $g_h$ or $g_a$. The effect of applying this assumption to the configuration used in this investigation

---

[36] Reese, op. cit.

may be seen more clearly in Figure 9 which is discussed further in the next chapter. It should also be emphasized - in case it is not already obvious to the reader - that the value of $g_h$ or $g_a$ for all fuel loading conditions, with the exception of the tank-empty condition, is a measure of not only structural damping but fluid damping as well.

## ANALYTICAL RESULTS

Flutter. The results of the analytical program are listed in Table IV in the same order as the experimental results listed in Table III. Since the tank was externally mounted, particular attention was directed to the effect of including oscillating aerodynamic forces and moments acting on the tank. The effect of damping is considered in the next chapter. For the fuel-loaded tank fixed at 40 per cent of the wing chord aft of the wing leading edge, linear superposition of the two-dimensional wing forces and the slender-body tank forces, according to the preceding section, reduced the flutter speed by 7 to 11 per cent. For the tank-empty configuration this reduction was increased from 7 per cent for a frequency ratio $\frac{\omega_h}{\omega_a}$ of 0.67 to 10 per cent for a frequency ratio of 1.13. When the empty tank was moved rearward to 60 per cent of the wing chord aft of the wing leading edge (see Table III(b), the inclusion of the tank forces

resulted in a reversed effect; that is, the flutter speed was increased by 10 per cent for nearly the same frequency ratio (see also Figure 8).

Divergence. As a matter of passing interest, stimulated by the fact that the model without fuel encountered divergence, rather than flutter, with the tank c.g. at 30 per cent of the wing chord aft of the wing leading edge, the effect of tank aerodynamic forces on the divergence speed was examined using the divergence speed equation given in the appendix. Recalling the force triangle shown in the introduction, notice the position divergence occupies outside the triangle between the aerodynamic and elastic forces. The implication is that this phenomenon is a static instability which is indeed the case. Specifically, static aeroelastic divergence of a lifting surface is an unstable condition in which the aerodynamic and elastic forces interact to give static deflections or displacements which are large enough to cause distortion or failure of the structure of the lifting surface. When the inertial terms are omitted from both the mechanical and aerodynamic parts of the equilibrium equations of motion for flutter, the unknown in the stability equation becomes a function only of velocity (V), and the solution of the reduced equation yields the velocity at which the surface will diverge, commonly known as the divergence speed.

Although in general both bending and torsional displacements must be considered, the type of divergence encountered here is known as torsional divergence since, as has been previously noted, the chordwise sections of both wing and tank are considered rigid, and only the torsional displacement (equivalent to the pitch angle or angle of attack which are, of course, identical in this investigation) is involved. Consequently, as illustrated in the appendix, the torsional divergence speed is found by restricting attention to equations involving $\alpha_j$ ($\alpha_1$ in this case).[37]

Results of the divergence speed calculations are presented in Table IV(b) alongside the flutter speeds and are also shown in Figure 8. As can be seen, the calculated divergence speeds obtained by including tank forces are approximately 10 per cent lower than those obtained by neglecting tank forces.

---

[37] Considerable work on divergence has been done by Franklin W. Diederich of the NACA Langley Laboratory, and for further information the reader is referred to any of his papers on this subject, as, for example, Divergence of Delta and Swept Surfaces in the Transonic and Supersonic Speed Ranges, NACA AGARD paper published April 1956.

# CHAPTER V

## CORRELATION OF THEORY AND EXPERIMENT

This chapter brings together the results of the experimental and theoretical parts of this investigation as presented in each of the two preceding chapters. In making the comparisons attention is directed to Figures 6, 8, and 9.

## GENERAL DISCUSSION

As can be seen in the figures just referred to, the use of effective values of mass and mass moment of inertia in the flutter calculations gave answers which agreed satisfactorily with experiment for nearly all fuel conditions. This result has also been obtained experimentally for this model in previously referenced studies[38] which show excellent agreement between the flutter speeds of the model with fluid and the flutter speeds of the model with solid weights equivalent to the fluid in effective mass and effective mass moment of inertia.

Neglect of aerodynamic forces and moments acting on the external tank led to calculated flutter speeds that were as much as 11 per cent unconservative (i.e., higher than experimental flutter speeds) for the fuel-loaded configuration

---

[38] Reese, op. cit.

(see Figure 6 for the tank 25 per cent full). With tank forces included, the calculations became generally conservative (i.e., calculated flutter speeds less than experimental flutter speeds). As can be seen, theory appears to follow closely the experimental trend up to the 95 per cent full condition, for which the calculated flutter speed was infinite whereas the experimental flutter speed was not.

Calculated flutter speeds were also conservative for the model in the empty condition with the tank center of gravity located at various chordwise positions ranging from 30 per cent to 60 per cent of the wing chord aft of the wing leading edge. As Figure 8 shows, the differences between calculated and experimental flutter speeds amounted to as much as 21 per cent. Furthermore, theory including tank aerodynamic forces exhibits a somewhat more consistent tendency to parallel experiment than does theory neglecting tank forces.

It can also be noted in Figure 8 that inclusion of tank forces resulted in a calculated divergence speed which agreed well with the experimental divergence speed for the tank at 30 per cent of the wing chord aft of the wing leading edge, but was 6 per cent less than the experimental flutter speed when the tank was at 40 per cent of the wing chord aft of the wing leading edge.

## SOME FURTHER REMARKS ON DAMPING

As noted in the previous chapter, the introduction of damping into flutter calculations by setting $g$ equal to the experimental values $g_h$ or $g_\alpha$ may be assumed to provide a flutter speed margin whose breadth depends on the trend of the theoretical $g$ value and the magnitude of $g_h$ or $g_\alpha$. However, as may be obvious to the reader, this assumption is valid only if the calculated flutter speed corresponding to the larger value of $g_h$ or $g_\alpha$ does not exceed the actual or experimental flutter speed. In many applications of flutter theory with damping accounted for in this manner the calculated flutter speeds are still conservative, but there are cases where use of this assumption leads to unconservative answers. Needless to say, this is an undesirable situation not only for the airplane manufacturer but also for the airplane pilot. It is just such a predicament that exists for the configuration studied in this present investigation.

Figure 9 shows $g$ as a function of flutter speed coefficient $\frac{V}{b\omega_\alpha}$ for all the tank fullnesses tested. As previously noted, the solid curves define theoretical borderline conditions between stable and unstable motion over a limited range of $g$ in the vicinity of the theoretical solution. Consistent with the assumption regarding damping,

the experimental flutter results from Table III(a) are positioned in Figure 9 according to experimental values of $g_h$ and $g_\alpha$. The points identified by the open circles represent speeds at which the borderline conditions between stable and unstable motion were first encountered experimentally. The solid circles represent experimental flutter speeds within the unstable region for all partially full conditions in which the flutter amplitudes were limited by fluid turbulence, as has already been discussed. The theoretical solutions at $g = 0$ correspond to the calculated flutter speed ratios presented in Figure 6 with tank aerodynamic forces and moments included.

It is important to note that the effect of damping appears to be more pronounced at the higher fuel loads, as is indicated by the consistent decrease in the slope of the theoretical curve. This behavior is attributed primarily to the fact that the frequency ratio passed through 1 as the tank fullness approached 100 per cent. The broken line shown in Figure 9(g) represents the stable condition (i.e., no flutter) shown in Figure 7 for a torsional component of the flutter amplitudes equal to $0^o$.

This sensitivity of theory to small amounts of damping was also typical of the cases of the empty-tank configuration tested with the tank in different chordwise positions.

Inclusion of damping according to the assumption $g = g_h$, which was less than $g_a$, resulted in flutter speeds that were unconservative by as much as 78 per cent with the tank center of gravity at 40 per cent of the wing chord aft of the wing leading edge.

# CHAPTER VI

## CONCLUSIONS

Analytical flutter studies were made for a two-dimensional fuel-loaded wing model, and the results are compared with experimental results for bending-to-torsion frequency ratios near 1. Water, simulating fuel, was carried externally in a geometrically scaled standard airplane fuel tank that was pylon-mounted a distance of about two and one-half times the tank radius beneath the wing. The results of the investigation appear to justify the following conclusions for this configuration:

1. The conclusion of previously referenced experimental studies[39] connected with the present investigation is herein reaffirmed analytically, namely, that effective values of mass and mass moment of inertia should be used in flutter calculations of fuel-loaded wings.

2. Inclusion of slender-body approximations to the aerodynamic forces and moments acting on the external tank at flutter tended to improve the agreement between flutter theory and experiment.

---

[39] Reese, op. cit.

3. Arbitrarily assuming the damping coefficient at flutter to be either $g_h$ or $g_\alpha$ gave calculated flutter speeds that were unconservative (or higher than experimental flutter speeds) by wide margins.

# BIBLIOGRAPHY

# BIBLIOGRAPHY


Ashley, H., G. Zartarian, and D. C. Neilson, Investigation of Certain Unsteady Aerodynamic Effects in Longitudinal Dynamic Stability, WADC ARTR 59-6, December 1951.

Barmby, J. G., H. J. Cunningham, and I. E. Garrick, Study of Effects of Sweep on the Flutter of Cantilever Wings, NACA Rep. No. 1014, 1951.

Beckley, Lawrence E., and H. Clay Johnson, Jr., An Experimental Investigation of the Flutter of a Tapered Wing With Simulated Engines, Tip Float and Tip Tank. (For the Bureau of Aeronautics, U. S. Navy), Massachusetts Institute of Technology, Contract No. NOa(s)7493, November 15, 1947.

Bisplinghoff, Raymond L., Holt Ashley, and Robert L. Halfman, Aeroelasticity, Addison-Wesley Publishing Company, Inc., 1955.

Clevenson, S. A., L. Widmayer, Jr., and Franklin W. Diederich, An Exploratory Investigation of Some Types of Aeroelastic Instability of Open and Closed Bodies of Revolution Mounted on Slender Struts, NACA TN 3308, November 1954.

Collar, A. R., The Expanding Domain of Aeroelasticity, Journal of the Royal Aeronautical Society, Vol. L, August 1946.

Diederich, Franklin W., Divergence of Delta and Swept Surfaces in the Transonic and Supersonic Speed Ranges, NACA AGARD paper, April 1956.

Gayman, William H., An Investigation of the Effect of a Varying Tip-Weight Distribution on the Flutter Characteristics of a Straight Wing, Journal of the Aeronautical Sciences, Vol. 19, No. 5, May 1952.

Graham, E. W., The Forces Produced in a Rectangular Tank, Douglas Aircraft Co., Inc., Report SM-13748, April 1951.

Graham, E. W., and A. M. Rodriguez, The Characteristics of Fuel Motion Which Affect Airplane Dynamics, Douglas Aircraft Co., Inc., Santa Monica, California, Report SM-14212, November 27, 1951.

Lamb, Sir Horace, Hydrodynamics, 6th ed., Dover Publications (New York), 1945.

Lorell, Jack, Forces Produced by Fuel Oscillations, Jet Propulsion Laboratory, California Institute of Technology, Progress Report No. 20-149, October 16, 1951.

Luskin, Harold, and Ellis Lapin, An Analytical Approach to the Fuel Sloshing and Buffeting Problems of Aircraft, Douglas Aircraft Co., Inc., Report SM-14068, June 1951.

Merten, Kenneth F., and Bertrand H. Stephensen, Some Dynamic Effects of Fuel Motion in Simplified Model Tip Tanks on Suddenly Excited Bending Oscillations, Langley Aeronautical Laboratory, NACA TN 2709, September 1952.

Miles, John W., An Analogy Among Torsional Rigidity, Rotating Fluid Inertia, and Self-Inductance for an Infinite Cylinder, Journal of Aeronautical Sciences, Vol. 13, No. 7, July 1946.

Reese, James R., Some Effects of Fluid in Pylon-Mounted Tanks on Flutter, Langley Aeronautical Laboratory, NACA RM L55F10, July 19, 1955.

Reese, James R., and John L. Sewall, Effective Moment of Inertia of Fluid in Offset, Inclined, and Swept-Wing Tanks Undergoing Pitching Oscillations, Langley Aeronautical Laboratory, NACA TN 3353, January 1955.

Scanlan, Robert H., and Robert Rosenbaum, Introduction to the Study of Aircraft Vibration and Flutter, MacMillan Co., 1951.

Schy, Albert A., A Theoretical Analysis of the Effects of Fuel Motion on Airplane Dynamics, NACA TN 2280, January 1951.

Scruton, C., Wing Flexure-Aileron Flutter Tests on a Model B.A.C. Wing Type 167, Aeronautical Research Council, R. and M. No. 2480, October 16, 1944.

Smilg, Benjamin, and Lee S. Wasserman, Application of Three-Dimensional Flutter Theory to Aircraft Structures, AFTR 4798, Materiel Div., Army Air Corps, July 9, 1942.

Theodorsen, Theodore, General Theory of Aerodynamic Instability and Mechanism of Flutter, NACA Rept. 496, 1935.

Theodorsen, Theodore, and I. E. Garrick, Mechanism of Flutter, A Theoretical and Experimental Investigation of the Flutter Problem, NACA Rept. No. 685, 1940.

Widmayer, Edward, Jr., and James R. Reese, Moment of Inertia and Damping of Fluid in Tanks Undergoing Pitching Oscillations, Langley Aeronautical Laboratory, NACA RM L53E01a, June 11, 1953.

# APPENDIX

## APPENDIX

## FLUTTER AND DIVERGENCE EQUATIONS FOR TWO-DIMENSIONAL WING CONFIGURATION INCLUDING AN EXTERNAL FUEL TANK

The analytical results presented in the main body of this paper were obtained by use of the equations derived in this appendix. As previously noted, a Rayleigh-Ritz method of analysis was employed, and the aerodynamic forces and moments were approximated by a linear superposition of two-dimensional theory for the wing and slender-body theory for the external tank. The flutter equations are developed first and are followed by the derivation of the divergence speed equation.

As noted in Chapter IV, the equilibrium equation of motion of the model at flutter for each degree of freedom is given by Lagrange's equation which may be written in the form

$$\frac{d}{dt}\left(\frac{\partial L}{\partial \dot{q}_j}\right) - \frac{\partial L}{\partial q_j} = Q_j \qquad (7)$$

where $L$ is the Lagrangian which is the difference between the kinetic and potential energies of the system, $q_j$ is the generalized coordinate for the j-th degree of freedom, and $Q_j$ is the generalized force corresponding to the j-th degree

of freedom. The dot over $q_j$ in this and subsequent equations represents the derivative with respect to time.

## FLUTTER

Derivation of the Lagrangian. As noted in chapter IV, the two-dimensional characteristics of the model and apparatus, as illustrated in Figure 2, reduced the flutter mode representation to a very simple form given by the natural vibration modes $h_1$ and $\alpha_1$ which are, respectively, rigid vertical translation (equivalent to bending) and rigid angular rotation or pitch (equivalent to torsion).[40]

Assuming small values of $h_1$ and $\alpha_1$ consistent with the concept of linear theory and considering $h_1$ as positive down and $\alpha_1$ as positive for leading edge up, the instantaneous position of the model is shown in the following sketch:

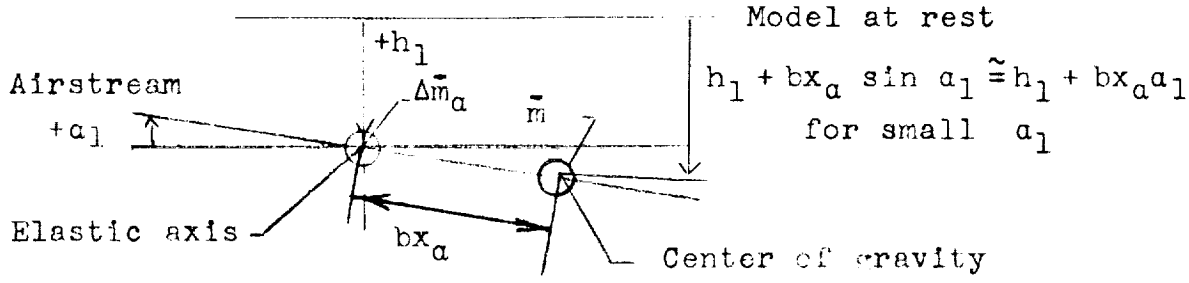


[40] See equations (5a) and (6a).

where $\Delta\bar{m}_a$ is the mass of the torsional springs (see Figure 2) and $\bar{m}$ is the mass of the model in pitch, that is

$$\bar{m} = \int_{\text{Span}} m\, dy + \bar{m}_T = ms + \bar{m}_T$$

where the integral applies to the wing, $s$ is the wing span, and $\bar{m}_T$ is the mass of the external tank. For the mass moment of inertia of the model about the center of gravity,

$$\bar{I}_o = \int_{\text{Span}} I_o\, dy + \bar{I}_{oT} = I_o s + \bar{I}_{oT}$$

where, similarly, the integral applies to the moment of inertia of the wing about the center of gravity, and $\bar{I}_{oT}$ is the moment of inertia of the external tank about the center of gravity.

Denoting the kinetic energy by $T$ and the potential energy by $U$,

$$L \equiv T - U = \frac{1}{2}\bar{m}\left(\dot{h}_1 + bx_a\dot{\alpha}_1\right)^2 + \frac{1}{2}\left(\Delta m_a\right)\dot{h}_1^2 + \frac{1}{2}\bar{I}_o\dot{\alpha}_1^2 - \frac{1}{2}\left[\left(1 + ig_h\right)k_h h_1^2 + \left(1 + ig_\alpha\right)k_\alpha \alpha_1^2\right] \qquad (8)$$

which, after expanding and combining certain inertial terms, becomes

$$L = \frac{1}{2}\bar{m}'\dot{h}_1^2 + \bar{m}bx_a\dot{h}_1\dot{a}_1 + \frac{1}{2}\bar{I}_a\dot{a}_1^2 -$$

$$\frac{1}{2}\left[\left(1 + ig_h\right)k_h h_1^2 + \left(1 + ig_a\right)k_a a_1^2\right] \qquad (8a)$$

where $\bar{m}' = \bar{m} + \Delta\bar{m}_a$, $\bar{I}_a = \bar{I}_o + \left(bx_a\right)^2\bar{m}$, $g_h$ is the translational damping coefficient, and $g_a$ is the pitching damping coefficient.

As noted in chapter IV, the value of $g_h$ or $g_a$ is considered as a measure of the combined structural and fluid damping for all fuel loadings. If the fluid in the model is regarded as having an effect on the structural damping coefficient, then it seems reasonable to apply the structural damping concept commonly used in flutter theory to cases involving fuel loads as well. While in the solution of natural vibration problems, damping is usually introduced as a force proportional to the velocity of the oscillations (i.e., the frequency), the type of damping important in classical flutter is a function of stiffness rather than frequency.[41] As pointed out by Scanlan and Rosenbaum,[42] this type of damping, known as either structural damping or structural friction, may be introduced into the flutter

---

[41] For further discussion on this matter see Theodorsen and Garrick, op. cit.

[42] Scanlan and Rosenbaum, op. cit.

analysis either by defining dissipation functions, which would appear in the generalized force $Q_j$, or by prefixing to the stiffness terms the quantities $1 + ig_h$ for the bending mode and $1 + ig_a$ for the torsional mode, as has been done in equations (8) and (8a) above.

Derivation of the generalized forces and moments. The generalized force $Q_j$ corresponding to the generalized coordinate $q_j$ is defined according to the principle of virtual work as $Q_j = \frac{\delta W}{\delta q_j}$ where $\delta W$ is the virtual work done by the force moving through a virtual or possible displacement $\delta q_j$ which is an infinitesimal displacement that does not violate the constraints of the system. According to this principle, if a given system is in equilibrium, the condition that it remain in equilibrium under the action of various forces, which can be inertial forces as well as static forces in accordance with D'Alembert's Principle, is that

$$\delta W = \sum_j Q_j \delta q_j = 0$$

Applying this condition to the present wing-tank configuration,

$$\delta W = Q_h \delta h_1 + Q_a \delta a_1 = 0 \qquad (9)$$

where $Q_h$ and $Q_\alpha$ are the external force and moment given by, respectively, the aerodynamic forces and moments acting on the wing and external tank. The sum of the products of $Q_h$ and $Q_\alpha$ by the virtual displacements $\delta h_1$ and $\delta \alpha_1$, respectively, through which these quantities move, gives the virtual work which must be zero so as not to violate the constraints of the system.

The unsteady aerodynamic forces and moments acting on the wing and external tank are shown in the following sketch of the instantaneous position of the configuration:

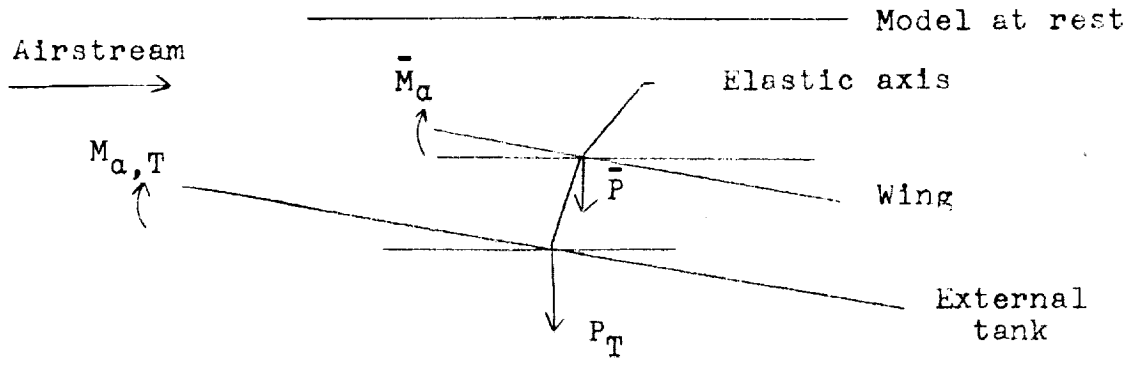


Thus, using equation (9),

$$Q_h = \frac{\delta W}{\delta h_1} = \bar{P} + P_T \quad \text{and} \quad Q_\alpha = \frac{\delta W}{\delta \alpha_1} = \bar{M}_\alpha + M_{\alpha,T} \tag{10}$$

where

$$\bar{P} = \int_{\text{Span}} \bar{P}\, dy = Ps \quad \text{and} \quad \bar{M}_\alpha = \int_{\text{Span}} M_\alpha\, dy = M_\alpha s$$

in terms of the two-dimensional aerodynamic force $P$ and moment $M_a$ on each spanwise strip of the wing. Expressions for $P$, $M_a$, $P_T$, and $M_{a,T}$ are presented later on in this development.

General form of equilibrium equations. Employing $h_1$ and $\alpha_1$ as generalized coordinates in equation (7) leads to the simultaneous equations

$$\frac{d}{dt}\left(\frac{\partial L}{\partial \dot{h}_1}\right) - \frac{\partial L}{\partial h_1} = Q_h \tag{7a}$$

and

$$\frac{d}{dt}\left(\frac{\partial L}{\partial \dot{\alpha}_1}\right) - \frac{\partial L}{\partial \alpha_1} = Q_\alpha \tag{7b}$$

Substitution of equations (8a) and (10) in equations (7a) and (7b) (after performance of the mathematical operations indicated in equations (7a) and (7b)) results in the following equilibrium equations of motion of the wing-tank configuration subjected to unsteady aerodynamic forces and moments:

$$\bar{m}'\ddot{h}_1 + \bar{m}bx_\alpha\ddot{\alpha}_1 + \left(1 + ig_h\right)k_h h_1 - \left(\bar{P} + P_T\right) = 0 \tag{11}$$

$$\bar{I}_\alpha\ddot{\alpha}_1 + \bar{m}bx_\alpha\ddot{h}_1 + \left(1 + ig_\alpha\right)k_\alpha\alpha_1 - \left(\bar{M}_a + M_{a,T}\right) = 0 \tag{12}$$

Imposing the condition of simple harmonic motion,[43] attention is restricted to solutions of these equations of the form $h_1 = h_{1,o}e^{i\omega t}$ for translation and $\alpha_1 = \alpha_{1,o}e^{i\omega t}$ for pitch. Substitution of these expressions into equations (11) and (12) results in

$$-\bar{m}'\omega^2 h_1 - \bar{m}bx_\alpha\omega^2\alpha_1 + \left(1 + ig_h\right)k_h h_1 - \left(\bar{P} + P_T\right) = 0 \qquad (11a)$$

$$-\bar{I}_\alpha\omega^2\alpha_1 - \bar{m}bx_\alpha\omega^2\alpha_1 + \left(1 + ig_\alpha\right)k_\alpha\alpha_1 - \left(\bar{M}_\alpha + M_{\alpha,T}\right) = 0 \qquad (12a)$$

for the general form of the equilibrium equations at flutter. At this point, it may be of interest to note that when $\bar{P} = P_T = \bar{M}_\alpha = M_{\alpha,T} = 0$, these equations can be solved for two values of $\omega$ which will be the coupled frequencies, both involving the $h$ and $\alpha$ components of the system at zero airspeed.[44]

Aerodynamic forces and moments on the wing. Expressions for $P$ and $M_\alpha$ appearing in equation (10) are those derived by Theodorsen[45] for two-dimensional, incompressible,

---

[43] This assumption is consistent with oscillatory type of motion implied in the borderline condition between stable and unstable motion. See Theodorsen, op. cit.

[44] This neglects the effects of stationary (or ambient) air surrounding the system at rest.

[45] Theodorsen, op. cit.

potential flow. Omitting consideration of the aileron, these expressions may be written in terms of $h_1$ and $\alpha_1$ as follows:

$$P = -\pi\rho b^2\left(V\dot{\alpha}_1 + \ddot{h}_1 - ba\ddot{\alpha}_1\right) - 2\pi\rho Vb(F + iG)\left[V\alpha_1 + \dot{h}_1 + b\left(\frac{1}{2} - a\right)\dot{\alpha}_1\right] \tag{13}$$

$$M_\alpha = -\pi\rho b^2\left[\left(\frac{1}{2} - a\right)Vb\dot{\alpha}_1 + b^2\left(\frac{1}{8} + a^2\right)\ddot{\alpha}_1 - ab\ddot{h}_1\right] + 2\pi\rho b^2V\left(a + \frac{1}{2}\right)(F + iG)\left[V\alpha_1 + \dot{h}_1 + b\left(\frac{1}{2} - a\right)\dot{\alpha}_1\right] \tag{14}$$

where $\rho$ is the mass-density of the airstream, $b$ is the wing half-chord, $a$ is the dimensionless distance of the elastic axis relative to the wing mid-chord, and $F$ and $G$ identify the circulatory portions of the aerodynamic forces and moments.[46] Again, since the model is assumed to be oscillating simusoidally, $\dot{h}_1 = i\omega h_1$, $\dot{\alpha}_1 = i\omega\alpha_1$, $\ddot{h}_1 = -\omega^2 h_1$, and $\ddot{\alpha}_1 = -\omega^2\alpha_1$, whence equations (13) and (14) may be written in the form

---

[46] $F$ and $G$ are given in terms of Bessel functions of the first and second kind and of zero and first order in equations (XII) and (XIII), Ibid.

$$P = -\pi\rho b^3\omega^2\left[\frac{h_1}{b} A_{ch} + a_1 A_{ca}\right] \tag{13a}$$

$$M_a = -\pi\rho b^4\omega^2\left[\frac{h_1}{b} A_{ah} + a_1 A_{aa}\right] \tag{14a}$$

where

$$A_{ch} = -1 + i2(F + iG)\frac{V}{b\omega} = -1 - \frac{2G}{k} + i\frac{2F}{k}$$

$$A_{ca} = i\frac{V}{b\omega} + a + 2(F + iG)\left(\frac{V}{b\omega}\right)^2 + i2(F + iG)\left(\frac{1}{2} - a\right)\left(\frac{V}{b\omega}\right)$$

$$= a + \frac{2F}{k^2} - \frac{2G}{k}\left(\frac{1}{2} - a\right) + i\left[\frac{1}{k} + \frac{2G}{k^2} + \frac{2F}{k}\left(\frac{1}{2} - a\right)\right]$$

$$A_{ah} = a - i2(F + iG)\left(\frac{1}{2} + a\right)\left(\frac{V}{b\omega}\right)$$

$$= a + \frac{2G}{k}\left(\frac{1}{2} + a\right) - i\frac{2F}{k}\left(\frac{1}{2} + a\right)$$

$$A_{a\alpha} = i\left(\frac{1}{2} - a\right)\left(\frac{V}{b\omega}\right) - \left(\frac{1}{8} + a^2\right) - 2\left(\frac{1}{2} + a\right)(F + iG)\left(\frac{V}{b\omega}\right)^2 -$$

$$i2\left(\frac{1}{2} + a\right)(F + iG)\left(\frac{1}{2} - a\right)\left(\frac{V}{b\omega}\right)$$

$$= -\left(\frac{1}{8} + a^2\right) - \frac{2F}{k^2}\left(\frac{1}{2} + a\right) + \frac{2G}{k}\left(\frac{1}{4} - a^2\right) +$$

$$i\left[\frac{1}{k}\left(\frac{1}{2} - a\right) - \frac{2F}{k}\left(\frac{1}{4} - a^2\right) - \frac{2G}{k^2}\left(\frac{1}{2} + a\right)\right]$$

and $\frac{1}{k} \equiv \frac{V}{b\omega}$ which is known as the reduced wave length.[47]

Aerodynamic forces and moments on the external tank. The oscillating aerodynamic forces and moments acting on the external tank are essentially identical to those derived by application of slender-body theory in a previous and somewhat

---

[47] The expressions for $A_{ch}$, $A_{c\alpha}$, $A_{ah}$, $A_{a\alpha}$ are identical to those given by Barmby, Cunningham, and Garrick in Study of Effects of Sweep Cantilever Wings, NACA Rep. No. 1014, 1951.

related investigation.[48] As noted in chapter IV, this theory is based on the assumption that the flow normal to the airstream is two-dimensional, and this assumption requires that the external tank be long and slender (i.e., have a high fineness ratio). From Tables I and II the length to maximum diameter gives a fineness ratio of 7.13 which is high enough for the external tank to be considered a slender body so that the theory was applicable.[49]

The application of slender-body theory begins with the determination of the momentum, in a direction normal to the airstream, of the virtual, or apparent mass, which may be defined as the mass of air displaced by a finite length of the body accelerating in this direction. For a body of revolution the apparent mass for an element dx of the body is simply $\pi\rho r^2(x)dx$. For the external tank of the present

---

[48] S. A. Clevenson, E. Widmayer, Jr., and Franklin W. Diederich, An Exploratory Investigation of Some Types of Aeroelastic Instability of Open and Closed Bodies of Revolution Mounted on Slender Struts, NACA TN 3308, November 1954 in the appendix for closed bodies of revolution. In this derivation the length along the body is measured aft of the nose of the body, whereas in the present paper the origin is chosen at the quarter-chord of the wing, as is shown in this section.

[49] This statement is based on the work of H. Ashley, G. Zartarian, and D. O. Neilson, namely, Investigation of Certain Unsteady Aerodynamic Effects in Longitudinal Dynamic Stability, WADC AFTR 5986, December 1951, in which the range of fineness ratios for which slender-body theory is considered valid is discussed.

configuration, at any station x on the body the total normal velocity is $\dot{h}_1 + V\alpha_1 + (x - e_a)\dot{\alpha}_1$ in terms of the translational velocity of and the pitching velocity about the wing elastic axis, together with the free-stream component due the pitching displacement $\alpha_1$. The orientation of these velocities is shown in the following sketch, the directions of the velocities being considered positive as shown:

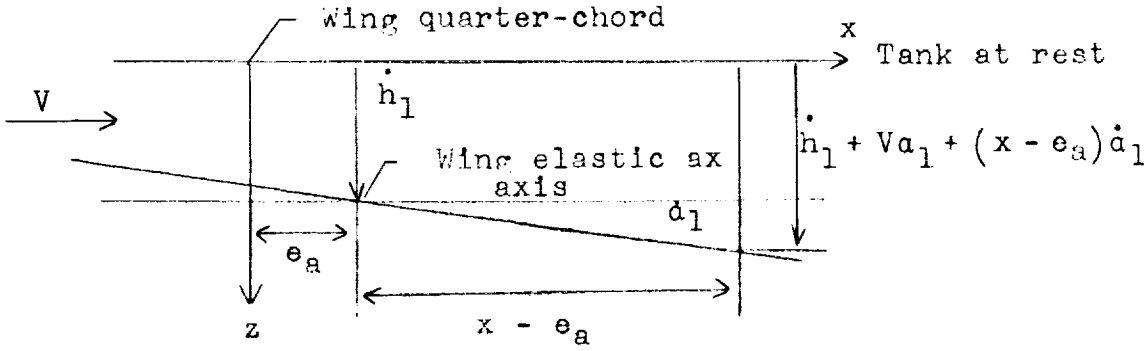


Denoting the momentum, per unit length, of flow perpendicular to the tank by $I_z$

$$I_z = \pi\rho r^2(x)\left[\dot{h}_1 + V\alpha_1 + (x - e_a)\dot{\alpha}_1\right] \qquad (15)$$

According to Newton's second law of motion, the force per unit length is equal to the time rate of change of the momentum, and since $I_z$ is a function of both $x$ and time,

$$\frac{dI_z}{dt} = -\left(\frac{\partial I_z}{\partial x}\frac{dx}{dt} + \frac{\partial I_z}{\partial t}\right) = -V\left(\frac{\partial I_z}{\partial x} + \frac{\partial I_z}{\partial t}\right) \qquad (16)$$

where the negative sign indicates that the air opposes the acceleration of the tank in the positive directions indicated in the foregoing sketch. Substitution of equation (15) into equation (16) results in

$$\frac{dI_z}{dt} = -\pi\rho V\left[\dot{h}_1 \frac{d}{dx} r^2(x) + Va_1 \frac{d}{dx} r^2(x) + \dot{a}_1 (x - e_a)\frac{d}{dx} r^2(x) + \dot{a}_1 r^2(x)\right] - \pi\rho r^2(x)\left[\frac{d\dot{h}_1}{dt} + V\dot{a}_1 + (x - e_a)\frac{d\dot{a}_1}{dt}\right] \tag{16a}$$

Imposing the requirement of simple harmonic motion, as before, and integrating over the length of the tank to obtain, respectively, the total oscillating aerodynamic force and moment about the elastic axis of the wing,

$$P_T = \int_{Tank} \frac{dI_z}{dt}\, dx = \rho V_T \omega^2 h_1 - \rho V_T \omega^2 a_1 \left(e_a - e_T + i\,\frac{b}{k}\right) \tag{17}$$

and

$$M_{a,T} = \int_{Tank} \frac{dI_z}{dt}(x - e_a)\,dx = \rho V_T \omega^2 h_1 \left(e_T - e_a + i\,\frac{b}{k}\right) + \rho\omega^2 a_1 \left(I_{T,a} + \frac{b^2}{k^2} V_T\right) \tag{18}$$

where

$$V_T = \int_{Tank} \pi r^2(x)dx$$

$$e_T = \frac{1}{V_T} \int_{Tank} \pi x r^2(x)dx$$

$$I_{T,a} = \int_{Tank} \pi (x - e_a)^2 r^2(x)dx$$

and the integrals

$$\int_{Tank} \frac{d}{dx} r^2(x)dx = \left[r^2(x)\right]_{Tank} = 0$$

$$\int_{Tank} (x - e_a) \frac{d}{dx} r^2(x)dx = \left[(x - e_a)r^2(x) - \int r^2(x)dx\right]_{Tank}$$

$$= - \int_{Tank} r^2(x)dx$$

and

$$\int_{Tank} (x - e_a)^2 \frac{d}{dx} r^2(x)dx = \left[(x - e_a)^2 r^2(x) - 2 \int (x - e_a) r^2(x)dx\right]_{Tank}$$

$$= -2 \int_{Tank} (x - e_a) r^2(x)dx$$

since the integration covers the length of the tank.

Derivation of the stability equations. If equations (13a), (14a), (17), and (18) are substituted into equations (11a) and (12a), and if Rayleigh type approximations are introduced in terms of the uncoupled frequencies given by $\omega_{h_1}^2 = \frac{k_h}{m'}$ and $\omega_{\alpha_1}^2 = \frac{k_\alpha}{I_\alpha}$, the equilibrium equations of motion of the wing-tank configuration at flutter can be obtained in the following compact form after performance of certain algebraic manipulations and introduction of certain dimensionless parameters which will be defined shortly:

$$A_{11} \frac{h_1}{b} + B_{11}\alpha_1 = 0 \tag{11b}$$

$$D_{11} \frac{h_1}{b} + E_{11}\alpha_1 = 0 \tag{12b}$$

where $A_{11}$, $B_{11}$, $D_{11}$, and $E_{11}$ represent the aerodynamic, inertial, and elastic forces interacting at flutter and where, in addition, the unknown frequency and damping coefficient are contained in $A_{11}$ and $E_{11}$. The condition that there exist solutions for $\frac{h_1}{b}$ and $\alpha_1$, other than the trivial solution $\frac{h_1}{b} = \alpha_1 = 0$, is that the determinant of the coefficients of $\frac{h_1}{b}$ and $\alpha_1$ shall vanish. Thus, for each value of $\frac{1}{k}$,

$$\begin{vmatrix} A_{11}B_{11} \\ D_{11}E_{11} \end{vmatrix} = 0 \qquad (19)$$

which leads to the flutter condition. Detailed expressions for the determinant elements are

$$A_{11} = \left(1 - \omega_{h_1}{}^2\Omega\right)\frac{1}{\kappa'} - \left(A_{ch} + A_{ch_T}\right)$$

$$B_{11} = \frac{x_\alpha{}'}{\kappa} - \left(A_{c\alpha} + A_{c\alpha_T}\right)$$

$$D_{11} = \frac{x_\alpha}{\kappa} - \left(A_{ah} + A_{ah_T}\right)$$

$$E_{11} = \left(1 - \omega_{\alpha_1}{}^2\Omega\right)\frac{r_\alpha{}^2}{\kappa} - \left(A_{a\alpha} + A_{a\alpha_T}\right)$$

where $\Omega = \frac{1}{\omega^2}(1 + ig)$, the dimensionless parameters previously mentioned are $\kappa' = \frac{\pi\rho b^2 s}{\bar{m}'}$, $x_\alpha{}' = \frac{\bar{m}}{\bar{m}'} x_\alpha$, $\kappa = \frac{\pi\rho b^2 s}{\bar{m}}$,

$r_a^2 = \frac{\bar{I}_a}{\bar{m}b^2}$, and where the aerodynamic coefficients for the external tank are given by

$$A_{ch_T} = -\frac{V_T}{\pi b^2 s}$$

$$A_{ca_T} = -A_{ch_T}\left(\frac{e_a - e_T}{b} + i\frac{1}{k}\right)$$

$$A_{ah_T} = A_{ch_T}\left(\frac{e_T - e_a}{b} + i\frac{1}{k}\right)$$

$$A_{aa_T} = -\frac{I_{T,a}}{\pi b^4 s} + A_{ch_T}\frac{1}{k^2}$$

## DIVERGENCE

As noted in chapter IV, torsional divergence is defined as a static aeroelastic instability involving only the torsional (pitching in this case) displacement of the elastic body being considered. In applying this definition to the wing-tank configuration studied in this paper, $h_1$ and $\omega$ are set equal to zero, whence $F + iG$ approaches unity as

$\frac{1}{k}$ becomes infinite,[50] and the flutter equations developed in the preceding section reduce to

$$r_a^2\omega_{a_1}^2 - \frac{2\pi\rho V^2 s}{m}\left(a + \frac{1}{2}\right) - \frac{\rho V^2 V_T}{\bar{m}b^2 s} = 0 \qquad (20)$$

which, when solved for V, gives the divergence speed

$$V \equiv V_d = b\omega_a\sqrt{\frac{r_a^2}{\kappa}\,\frac{1}{2\left(a + \frac{1}{2}\right) - A_{ch_T}}} \qquad (21)$$

The divergence speeds presented in the main body of this paper were calculated by means of this equation.[51]

---

[50] Theodorsen, op. cit., Figure 4.

[51] For the two-dimensional wing alone, that is $A_{ch_T} = 0$, this equation reduces to that given by Theodorsen and Garrick, op. cit.